

# International Conference on Space Optics—ICSO 2018

Chania, Greece

9–12 October 2018

*Edited by Zoran Sodnik, Nikos Karafolas, and Bruno Cugny*



## *Optical performance of the Metis coronagraph on the Solar Orbiter ESA mission*

*Fabio Frassetto*

*Vania Da Deppo*

*Paola Zuppella*

*Marco Romoli*

*et al.*



icso proceedings



International Conference on Space Optics — ICSO 2018, edited by Zoran Sodnik, Nikos Karafolas, Bruno Cugny, Proc. of SPIE Vol. 11180, 111806Y · © 2018 ESA and CNES · CCC code: 0277-786X/18/\$18 · doi: 10.1117/12.2536169

Proc. of SPIE Vol. 11180 111806Y-1

## Optical performance of the Metis coronagraph on the Solar Orbiter ESA mission

Fabio Frassetto<sup>a\*</sup>, Vania Da Deppo<sup>a,b</sup>, Paola Zuppella<sup>a</sup>, Marco Romoli<sup>c</sup>, Silvano Fineschi<sup>d</sup>, Ester Antonucci<sup>d</sup>, Giana Nicolini<sup>d</sup>, Giampiero Naletto<sup>e,a,b,f</sup>, Piergiorgio Nicolosi<sup>g</sup>, Daniele Spadaro<sup>h</sup>, Vincenzo Andretta<sup>i</sup>, Marco Castronuovo<sup>l</sup>, Marta Casti<sup>d</sup>, Gerardo Capobianco<sup>d</sup>, Giuseppe Massone<sup>d</sup>, Roberto Susino<sup>d</sup>, Federico Landini<sup>m</sup>, Maurizio Pancrazzi<sup>c</sup>, Luca Teriaca<sup>n</sup>, Udo Schuehle<sup>n</sup>, Klaus Heerlein<sup>n</sup>, Michela Uslenghi<sup>o</sup>

<sup>a</sup>CNR-IFN Padova, Via Trasea 7, 35131 Padova, Italy

<sup>b</sup>INAF-Osservatorio Astronomico di Padova, Vicolo dell'Osservatorio 5, 35122 Padova, Italy

<sup>c</sup>Dipartimento di Fisica ed Astronomia - Università degli Studi di Firenze, Via G. Sansone 1, 50019 Sesto Fiorentino (Fi), Italy

<sup>d</sup>INAF – Osservatorio Astrofisico di Torino, Strada Osservatorio 20, 10025 Pino Torinese (To), Italy

<sup>e</sup>Dipartimento di Fisica e Astronomia “Galileo Galilei” - Università degli Studi di Padova, Via Marzolo 8, 35131 Padova, Italy

<sup>f</sup>CISAS Centro Interdipartimentale Studi e Attività Spaziali “G. Colombo”, Via Venezia 15, 35131 Padova, Italy

<sup>g</sup>Dipartimento di Ingegneria dell'informazione, Università di Padova, Via Gradenigo 6/B, 35131 Padova, Italy

<sup>h</sup>INAF-Osservatorio Astrofisico di Catania, Via S. Sofia 78, 95123 Catania, Italy

<sup>i</sup>INAF-Osservatorio Astronomico di Capodimonte, Salita Moiariello 16, 80131 Napoli, Italy

<sup>l</sup>ASI, Via del Politecnico, 00133 Roma, Italy

<sup>m</sup>INAF-Osservatorio Astrofisico di Arcetri, Largo E. Fermi 5, 50125 Firenze, Italy

<sup>n</sup>Max Planck Institute for Solar System Research, Justus-von-Liebig-Weg 3, 37077 Göttingen, Germany

<sup>o</sup>INAF-IASF, Via E. Bassani, 20133 Milano, Italy

### ABSTRACT

The Metis coronagraph aboard the Solar Orbiter ESA spacecraft is expected to provide new insights into the solar dynamics. In detail, it is designed to address three main questions: the energy deposition mechanism at the poles (where the fast wind is originated), the source of the slow wind at lower altitude, and how the global corona evolves, in particular in relation to the huge plasma ejections that occasionally are produced. To obtain the required optical performance, not only the Metis optical design has been highly optimized, but the alignment procedure has also been subjected to an accurate evaluation in order to fulfill the integration specifications. The telescope assembling sequence has been constructed considering all the subsystems manufacturing, alignment and integration tolerances. The performance verification activity is an important milestone in the instrument characterization and the obtained results will assure the fulfillment of the science requirements for its operation in space.

The entire alignment and verification phase has been performed by the Metis team in collaboration with Thales Alenia Space Torino and took place in ALTEC (Turin) at the Optical Payload System Facility using the Space Optics Calibration Chamber infrastructure, a vacuum chamber especially built and tested for the alignment and calibration of the Metis coronagraph, and suitable for tests of future payloads.

The goal of the alignment, integration, verification and calibration processes is to measure the parameters of the telescope, and the characteristics of the two Metis channels: visible and ultraviolet. They work in parallel thanks to the peculiar optical layout. The focusing and alignment performance of the two channels must be well understood, and the results need

\*fabio.frassetto@pd.ifn.cnr.it; phone + 39 049 981 7447

to be easily compared to the requirements. For this, a dedicated illumination method, with both channels fed by the same source, has been developed; and a procedure to perform a simultaneous through focus analysis has been adopted.

In this paper the final optical performance achieved by Metis is reported and commented.

**Keywords:** Metis, solar orbiter, coronagraphy, space instrumentation, optical calibration

## 1. INTRODUCTION

The Metis coronagraph design is based on an “inverted externally occulted” configuration<sup>1-3</sup>. The entrance aperture (EA) acts as the telescope entrance pupil and the disk light rejecting optics, the M0 mirror, is inside the structure (see Figure 1). Metis combines a visible light (VL) channel, in the range 580-640 nm, and an ultraviolet (UV) channel at the HI Lyman  $\alpha$  at 121.6 nm. Both channels share the same imaging optics and the field of view (FOV) is 1.6° - 2.9°.

The telescope has a Gregorian configuration. Both the primary (M1) and secondary (M2) mirrors have annular shape. The telescope focal plane is outside the M1-M2 assembly. The arrangement is presented in Figure 1. An interferential filter assembly (IFA) separates the light acquired by the telescope into the two channels, and then the beams are focalized onto two different detectors. M0, mounted in front of M1, reflects the solar disk radiation back to the entrance aperture (EA).

The IFA reflects the VL radiation, which is focalized at an intermediate focal plane (IFP), and then re-imaged on the VL detector (VLDA) via the polarimetric module. This later consists in: the collimating doublet (CD), bandpass filter (BP), quarter-wave plate retarder (QW), polarization modulation package (PMP), linear polarizer (LP) and focusing lens system (FLS).

The UV radiation propagates through the IFA, and is focalized towards the M1-M2 focal plane. The real UV focal plane position is slightly shifted due to the 6-mm thick IFA and the 4-mm thick MgF<sub>2</sub> window mounted in front of the UV detector (UVDA).

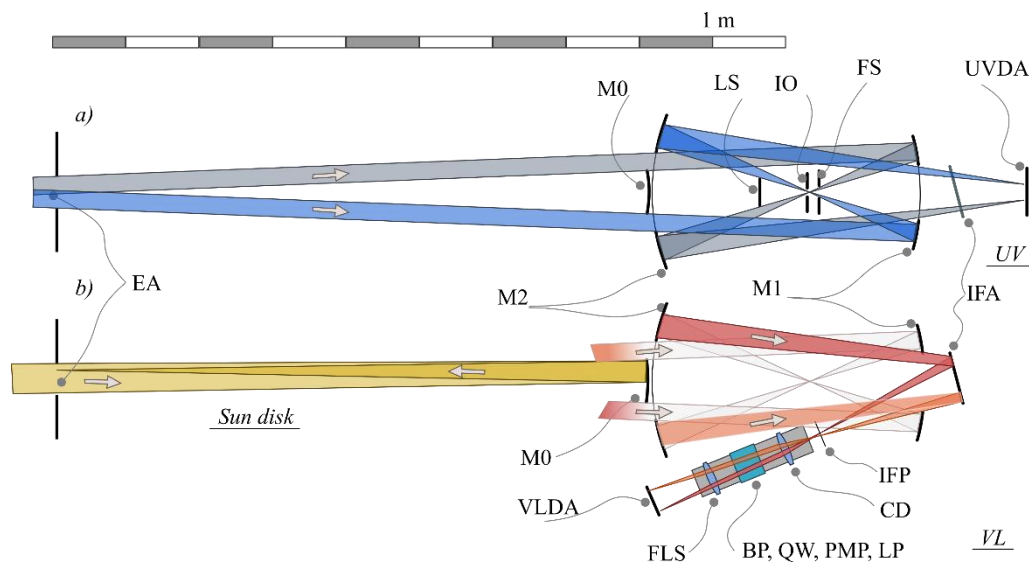


Figure 1. Metis optical layout. a) UV path. b) VL path and Sun disk rejection principle. LS Lyot stop; IO internal occulter; FS field stop.

The Metis alignment and calibration test set-up features different kinds of sources. A multiple collimated beam source has been used for assembling purpose. A multiple pinhole (point-like source) placed in the focal plane of a collimator has been used for the VL channel focus test; a single pinhole has been used for the combined UV and VL channel calibration. In the last case, the possibility of moving the point-like source along the optical path has permitted “through focus” measurements.

The combined analysis of the performance of both the VL and UV channels, carried out using a single source, is one of the peculiar solutions adopted during the calibration campaign. This procedure allows to disentangle possible environmental artifacts from the pure Metis behavior.

## 2. ALIGNMENT PROCEDURE

The alignment of a coronagraph profoundly differs from that of an unobstructed optical system; this is mainly due to the fact that the central part of its FOV is totally vignetted. This feature, peculiar to all the coronagraphs, precludes the use of straightforward alignment procedures. Figure 2 illustrates the major steps in the adopted alignment procedure for M1 and M2.

The assembling procedure pursues the following main steps<sup>4</sup>: at first M2 is mechanically integrated and the autocollimator (AC) collimated on the auxiliary reference surface (ARS) of M2, then the plane parallel plate (PPP) is positioned orthogonally to the autocollimator (ATC) (see Figure2(a)). The auxiliary sighting telescope (AST) is centered on the M2 target and orthogonally positioned with respect to the PPP (see Figure2(b)). The theodolite (THEO) is centered on M2 target and co-aligned with AST (see Figure2(c)). M1 is integrated and centered with THEO (see Figure2(d)). THEO is translated and the M1 is regulated so that its ARS is orthogonal to the THEO (see Figure2(e)).

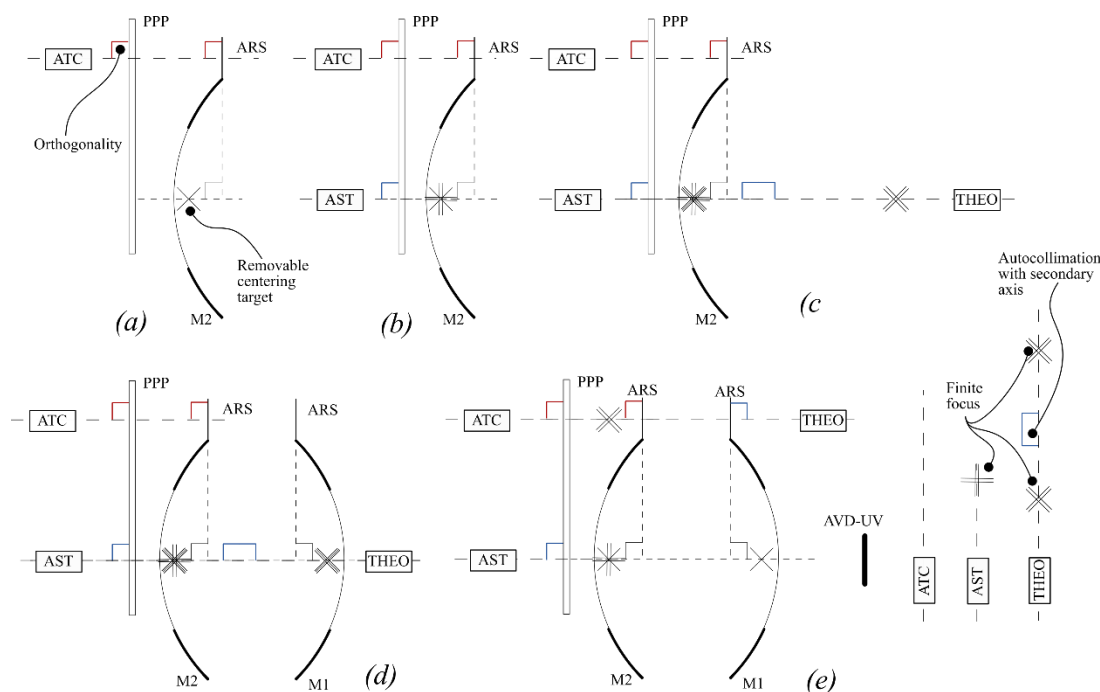


Figure 2. Scheme of the alignment procedure of M1 and M2. From (a) to (e) major steps of the alignment sequence.

The correct alignment between M1 and M2 is checked using an auxiliary detector placed at the UV focal plane (AVD-UV); the test was made taking into account the absence of both the interference filter assembly (IFA) element and the MgF<sub>2</sub> detector window. The distance between M1 and M2 determines the telescope focal length.

The alignment proceeds using an auxiliary alignment source (AAS)<sup>5</sup> (see Figure 3). The AAS feeds the telescope through the hole of M2. The nominal orientations of the AAS four collimated beams with the telescope axis are the  $\alpha_a, \alpha_b, \alpha_c, \alpha_d$  angles, which have a value of 2.5°. In Figure 3(b) the four collimated beams originating from the source are depicted. The four collimated beams act as four point-like sources placed “at infinity” inside the Metis FOV. In Figure 3(c) the alignment set up and the pattern at the AVD-UV plane are shown. “Da” indicates the distance of a generic point image from the point at which the optical axis intersects the AVD-UV plane, and it is used for the measurement of the plate scale factor (i.e. the conversion factor between the angle of the collimated beam with respect to the telescope axis and the image position at the focal plane).

Being the focal plane positions essentially fixed, for both the VL and the UV channels, (small adjustments were possible using shims), the proper M1 - M2 distance has been defined measuring two parameters on the AVD-UV: the spot quality and the image plate scale.

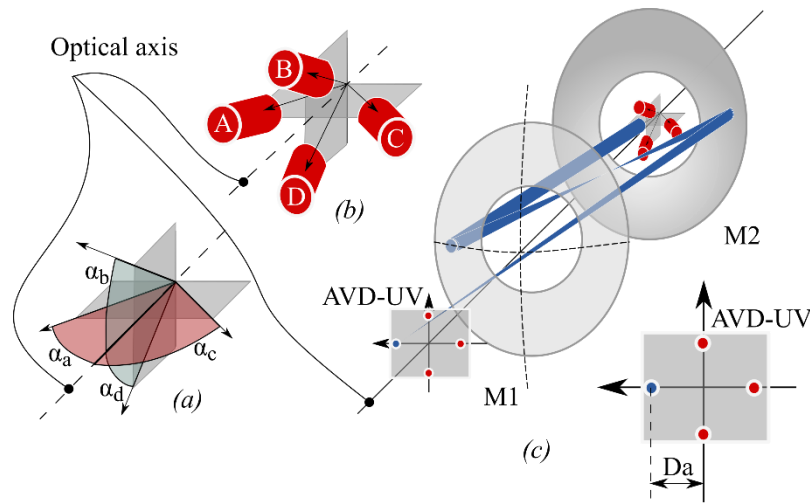


Figure 3. Alignment procedure making use of the AAS. In (a) and (b) orientation of the 4 AAS collimated beams. In (c) alignment set-up and pattern on the AVD-UV detector.

Finally, the IFA element and the VL channel have been integrated.

### 3. TEST FACILITY ASSEMBLY

The integration of Metis performed in the chamber of the Optical Payload System Facility<sup>6</sup> is shown in Figure 4. In a) schematics of the calibration arrangement of Metis; the effective focal length (EFL) and the angle  $\alpha$ , the angle between Metis optical axis and the collimated beam inside the FOV, are highlighted.

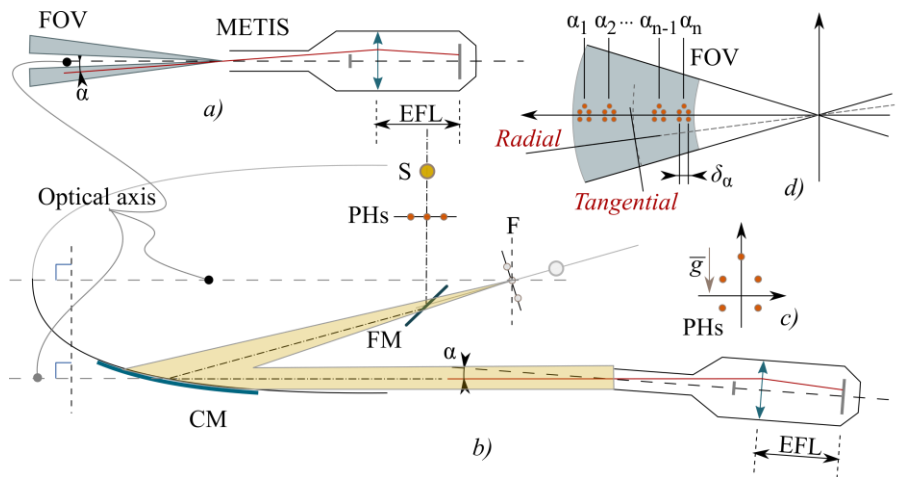


Figure 4. Integration of Metis at the Space Optics Calibration Chamber facility. a) Schematics of the calibration principle. b) Scheme of the calibration set-up. S is the source and F the focus of CM. c) PHs, pinholes assembly; d) Representation of the FOV sampling using the multiple pinhole mask.

In Figure 4b) the optical scheme of Metis in the test facility and the working principle of the collimating mirror (CM) off-axis parabola is clarified. This figure also explains the location of the pinholes: they are in the focal plane of the CM, considering the pivoting effect of the folding mirror (FM). The source (S) is white light or UV depending on the test phase. In c) the five pinholes (PHs) assembly, made up by five holes of 200  $\mu\text{m}$  in diameter, and its orientation with respect to

the gravity vector are depicted. The effect of changing the value of the angle “ $\alpha$ ” is detailed in Figure 3d). The position of the multiple pinhole mask inside the FOV for each  $\alpha_n$  is shown, the effect of  $\delta\alpha$  is neglected; also the radial and tangential directions are indicated.

For the tests involving the UV detector, the chamber has been operated in vacuum conditions.

In the next sections the results for the two channels, VL and UV, are presented.

#### 4. VISIBLE CHANNEL PERFORMANCE

As a first test, using the same AAS source used for the M1 and M2 alignment, the spot quality at the visible light focal plane has been measured. At this stage of the integration the IFA position has been adjusted to optimizing the spot quality. Only three of the four AAS spots are considered, the fourth being saturated.

The results are presented in Figure 5.

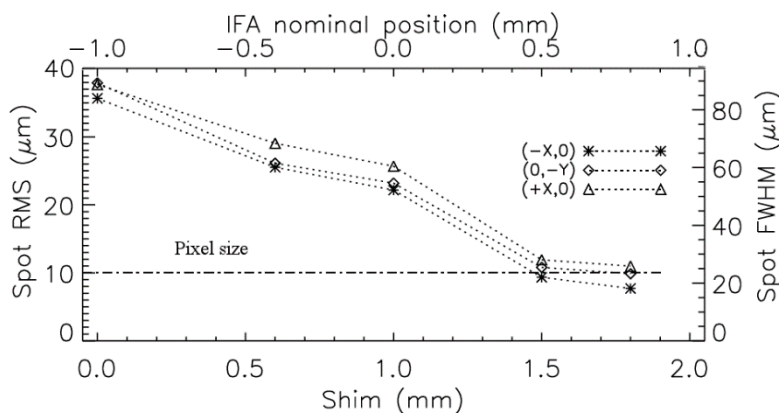


Figure 5. AAS spot quality at the VL focal plane. The RMS and FWHM of the spots are shown and compared with the pixel size.

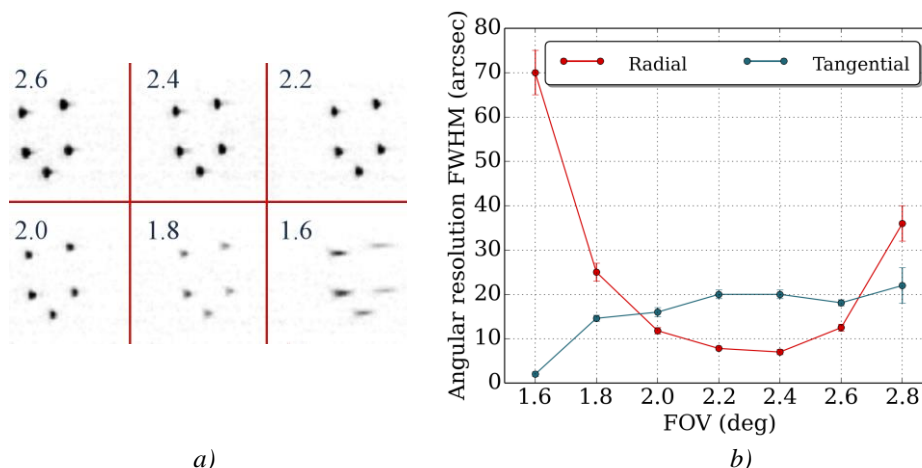


Figure 6. a) Spots of the VL channel for different values inside the FOV, the diffraction effect is clearly visible at the lowest FOV values. b) Metis measured angular resolution: radial and tangential values are reported.

By using the five 200  $\mu\text{m}$  pinholes target, successively the results summarized in Figure 6 have been obtained.

Given the ratio between the Metis VL channel focal length (200 mm) and the collimator focal length (about 2 m), the demagnification factor of the set-up is 0.098. Thus the expected geometric source dimension at the VL focal plane is 20  $\mu\text{m}$  (two pixels). This factor has been considered in the analysis.

The diffraction effects depend on the considered position in the FOV and on the considered direction: either radial or tangential. Radial is along the direction of a radius from the sun center, and tangential is the perpendicular one. In the inner portion of the FOV most of the rays in the beam are vignetted, the diffraction effects are high and the spots are elongated in the radial direction (see Figure 6).

A resolution of 20 arcsec is obtained in almost all the FOV.

## 5. UV CHANNEL PERFORMANCE

The characterization of the UV channel has been conducted replacing the visible light source with a Krypton lamp coupled to a UV filter. The multiple pinhole mask used in the VL test has been replaced with a single 25  $\mu\text{m}$  diameter pinhole. Examples of the acquired images are shown in Figure 7. The elongation of the images make evident the presence of some kind of aberrations. The radial and tangential measures are reported in Figure 8.

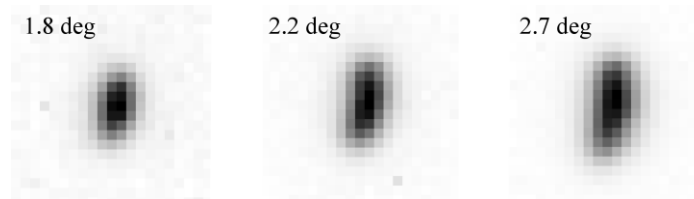


Figure 7. UV channel spot quality: pinhole images acquired for three different positions inside the FOV.

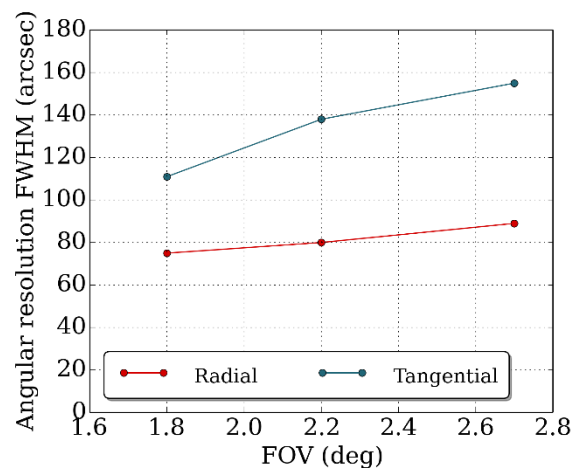


Figure 8. UV channel angular resolution as a function of the FOV.

Along the radial direction the resolving element is 80 arcsec, in agreement with the requirements, and almost constant in the 1.8° - 2.7° FOV; at minimum perihelion this correspond roughly to 15000 km. Along the tangential direction the resolution is lower than expected of a factor in the range 1.5 - 1.7.

## 6. VL AND UV THROUGH FOCUS MONITORING

In order to disentangle the effects of the test assembly, if any, to those eventually existing in Metis, a source containing both VL and UV light has been obtained by removing the spectral filter in front of the Krypton lamp. In this way not only UV photons, but also VL ones, can feed Metis at the same time and the two channels can be operated and tested in parallel.

Using the same single pinhole adopted for the (pure) UV channel characterization, a combined UV and VL characterization has been carried out. The two beams, UV and VL, have the same geometrical characteristics, and if there is an issue in the test set-up, e.g. aberration related to the source position, this has to affect both channels. The simplified optical scheme of the through-focus measurements for both the VL and UV channels is presented in Figure 9.

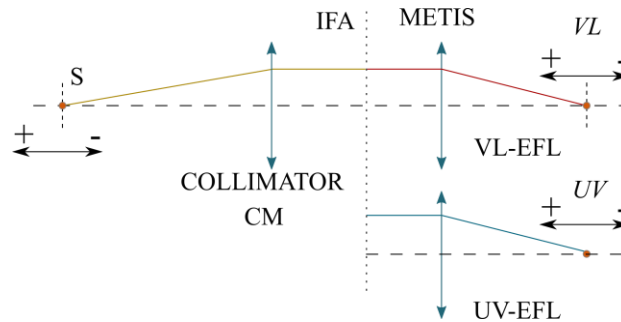


Figure 9. Through focus test scheme. The movement of the source *S* from its nominal position produces a movement of the image location. The relation between the movement direction of *S* and the correspondent motion of the image (both for the VL and UV channels) is clarified together with the adopted sign convention.

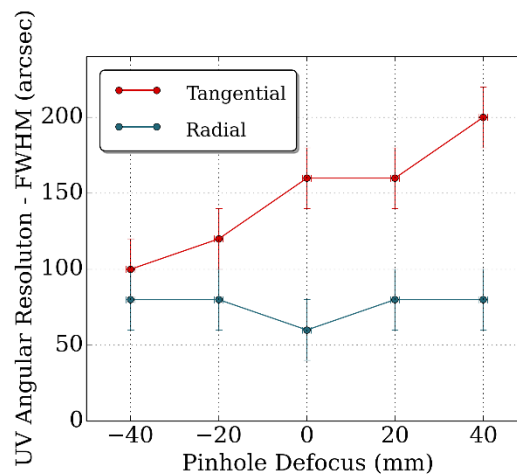


Figure 10. Measured UV spot quality when both channels are operated in parallel with a common point like source.

The results of these tests for the UV channel are presented in Figure 10. The corresponding results for the VL channel exclude an instrumental effect originated in the calibration set-up. Thus confirming the results presented in Section 5.

The attainable resolution in the tangential direction is affected by two concomitant effects: the UV detector is probably not in the nominal position, and the UV resolving element, in the tangential direction, is probably larger than expected. The Metis team is considering the use of a suitable deconvolution algorithm in order to partially recover the UV image quality.

## 7. CONCLUSIONS

In this paper the entire alignment and verification phase performed by the Metis team is described. The goal of the alignment, integration, verification and calibration processes was to measure the parameters of the telescope, and the characteristics of the two Metis channels. They work in parallel thanks to the peculiar optical layout.

A dedicated illumination method, with both channels fed by the same source, has been developed; and a procedure to perform a simultaneous through focus analysis has been adopted.



The obtained focus and through-focus results for both the UV and VL channels are described and discussed. The attainable resolution both in the radial and tangential directions in the VL channel complies with the specification. For the UV one the radial is as expected, while the attainable resolution in the tangential direction is affected by two concomitant effects: the UV detector is probably not in the nominal position, and the UV resolving element is probably larger than expected.

## ACKNOWLEDGMENTS

This work has been supported by the Italian Space Agency – ASI - under contract to the co-financing National Institute of Astrophysics (INAF) Accordo Addendum I/013/12/0 and under the contract to the industrial partners: ASI-ATI N. 2013-057-I.0.

ASI prime contractor for the Metis project has been OHB-CGS that delivered the opto-mechanical design, the electronics and the software. Thales Alenia Space Italy was responsible for the instrument integration and alignment activity. The VLDA assembly was provided by MPS under Contract 2013-058-I.0 with the Italian Space Agency (ASI). The UVDA assembly was provided by MPS as German contribution to Metis thanks also to the financial support of DLR (grant 50 OT 1201). The primary and secondary mirrors were provided as Czech contribution to Metis; the mirror hardware development was possible thanks to the Czech PRODEX Programme.

The authors thank the ALTEC Company for providing logistic and technical support.

The authors would like to thank the team of the Metis THALES Alenia Space - Italy for their support; in particular: S. Cesare, R. Boccardo, R. Brando, C. Baietto, R. Bertone, S. Mottini, and P. Sandri of OHB-Italia for the fruitful discussion on the telescope focus obtained results.

## REFERENCES

- [1] Fineschi, S., Antonucci, E., Naletto, G., Romoli M., Spadaro D., Nicolini G., Abbo L., Andretta V., Bemporad, A., Berlicki A., Capobianco, G., Crescenzo, G., Da Deppo, V., Focardi, M., Landini, F., Massone, G., Malvezzi, M. A., Moses, J. D., Nicolosi, P., Pancrazzi, M., Pelizzo, M.-G., Poletto, L., Schühle, U. H., Solanki, S. K., Telloni, D., Teriaca, L., Uslenghi, M., "METIS: a novel coronagraph design for the Solar Orbiter mission," Proc. SPIE 8443, Space Telescopes and Instrumentation 2012: Ultraviolet to Gamma Ray, 84433H (2012).
- [2] Romoli, M., Landini, F., Antonucci, E., Andretta, V., Berlicki, A., Fineschi, S., Moses, J. D., Naletto, G., Nicolosi, P., Nicolini, G., Spadaro, D., Teriaca, L., Baccani, C., Focardi, M., Pancrazzi, M., Pucci, S., Abbo, L., Bemporad, A., Capobianco, G., Massone, G., Telloni, D., Magli, E., Da Deppo, V., Frassetto, F., Pelizzo, M. G., Poletto, L., Uslenghi, M., Vives, S., Malvezzi, M., "METIS: the visible and UV coronagraph for solar orbiter," Proc. SPIE 10563, International Conference on Space Optics — ICSO 2014, 105631M (2017).
- [3] Landini, F., Vivès, S., Romoli M., Guillon, C., Pancrazzi, M., Escolle, C., Focardi, M., Antonucci, E., Fineschi, S., Naletto, G., Nicolini, G., Nicolosi, P., Spadaro, D., "Optimization of the occulter for the Solar Orbiter/METIS coronagraph," Proc. SPIE 8442, Space Telescopes and Instrumentation 2012: Optical, Infrared, and Millimeter Wave, 844227 (2012).
- [4] Da Deppo, V., et al., "Alignment procedure for the Gregorian telescope of the Metis coronagraph for the Solar Orbiter ESA mission," to be published in this Proc. SPIE volume, (2018).
- [5] Tordi, M., Bartolozzi, M., Fineschi, S., Capobianco, G., Massone, G., Cesare, S., "Illumination system in visible light with variable solar-divergence for the solar orbiter METIS coronagraph," Proc. SPIE 9604, Solar Physics and Space Weather Instrumentation VI, 96040V (2015).
- [6] Fineschi, S., Crescenzo, G., Massone, G., Capobianco, G., Zangrilli, L., Antonucci, E., Anselmi, F., "OPSys: optical payload systems facility for testing space coronagraphs," Proc. SPIE 8148, Solar Physics and Space Weather Instrumentation IV, 81480W (2011).